



# Nanocomposite scaffolds of bioactive glass ceramic nanoparticles disseminated chitosan matrix for tissue engineering applications

Mathew Peter<sup>a</sup>, N.S. Binulal<sup>a</sup>, S. Soumya<sup>a</sup>, S.V. Nair<sup>a</sup>, T. Furuike<sup>b</sup>, H. Tamura<sup>b</sup>, R. Jayakumar<sup>a,\*</sup>

<sup>a</sup> Amrita Centre for Nanosciences, Amrita Institute of Medical Sciences and Research Centre, Amrita Vishwa Vidyapeetham University, Kochi 682026, India

<sup>b</sup> Faculty of Chemistry, Materials and Bioengineering & High Technology Research Centre, Kansai University, Osaka 564-8680, Japan

## ARTICLE INFO

### Article history:

Received 1 July 2009

Received in revised form 22 July 2009

Accepted 3 August 2009

Available online 11 August 2009

### Keywords:

Tissue engineering

Chitosan

Bioactive glass ceramic nanoparticles

Nanocomposite scaffolds

Biomaterials

## ABSTRACT

A novel nanocomposite scaffold of chitosan (CS) and bioactive glass ceramic nanoparticles (nBGC) was prepared by blending nBGC with chitosan solution followed by lyophilization technique. The particle size of the prepared nBGC was found to be 100 nm. The prepared composite scaffolds were characterized using techniques such as Scanning Electron Microscopy (SEM), Fourier Transform Infrared Spectroscopy (FT-IR) and X-ray diffraction (XRD). The SEM studies showed that the bioactive nBGC were homogeneously distributed within the chitosan matrix. The swelling, density, degradation and *in-vitro* biomineralization studies of the composite scaffolds were also studied. The composite scaffolds showed adequate swelling and degradation properties. The *in-vitro* biomineralization studies confirmed the bioactivity nature of the composite scaffolds. Cytocompatibility of the composite scaffolds were assessed by MTT assay, direct contact test and cell attachment studies. Results indicated no toxicity, and cells attached and spread on the pore walls offered by the scaffolds. These results indicate that composite scaffolds developed using nBGC disseminated chitosan matrix as potential scaffolds for tissue engineering applications.

© 2009 Elsevier Ltd. All rights reserved.

## 1. Introduction

Bone tissue engineering is gaining popularity as alternative method for treatment of osseous defects. A number of biodegradable polymers have been explored for tissue engineering purposes. These include synthetic polymers like poly(caprolactone), poly(lactic-co-glycolic acid), poly(ethylene glycol), poly(vinyl alcohol) and natural polymers like alginate, collagen, gelatin, chitin, chitosan etc. (Hirano et al., 1990). Chitosan is a biopolymer derived from partial deacetylation of chitin. Chitosan is considered as an appropriate functional material for biomedical applications because of its high biocompatibility, biodegradability, non-antigenicity and protein adsorption properties (Gupta, Mahor, Khatri, Goyal, & Vyas, 2006; Jayakumar, Nwe, Tokura, & Tamura, 2007; Jayakumar, Prabhakaran, Reis, & Mano, 2005; Jayakumar, Reis, & Mano, 2006; Jayakumar, Selvamurugan, Nair, Tokura, & Tamura, 2008; Muzzarelli et al., 1988; Muzzarelli, 2009). CS favour cell adhesion due to its chemical backbone, which resembles glycosaminoglycans, a major component of bone and cartilage. However, continuous efforts are being made to improve the bioactivity & compatibility of chitosan along with better mechanical properties. Many inorganic materials are in the literature, like hydroxyapatite (Jayakumar & Tamura,

2006; Jiang, Nair, & Laurencen, 2006; Kong et al., 2005; Zhang et al., 2008; Zhao, Grayson, Ma, Bunnell, & Lu, 2006),  $\beta$ -TCP (Takahashi, Yamamoto, & Tabata, 2005; Yin et al., 2003) and montmorillonite (Zheng et al., 2007), which are added to improve the properties of chitosan.

Bioactive glass ceramic is a group of osteoconductive biomaterial used as bone repair materials. They are silicate glasses containing  $\text{SiO}_2$ – $\text{CaO}$ – $\text{P}_2\text{O}_5$  networks. This ceramic is known to bond to hard and soft tissues by the formation of surface hydroxy carbonate apatite (HCA) layer (Cao & Hench, 1996). Reports also suggest that bioactive glass ceramic influences the cell adhesion, proliferation, differentiation and colonization on surface of implants (Bosetti & Cannas, 2005; Verrier, Blaker, Maquet, Hench & Boccaccinia, 2004; Xynos, Edgar, Buttery, Hench, & Polak, 2000). Bioactive glass also allows the expression of peculiar osteoblast differentiation marker, namely osteocalcin (Foppiano, Marshall, Marshall, Saiz, & Tomsia, 2007; Oliva et al., 1998).

Nanosurface and nanoparticles are known to influence cell behaviour including attachment & spreading (Dalby, McCloy, Robertson, Wilkinson, & Oreffo, 2006; Lauer et al., 2001; Linez-Bataillon, Monchau, Bigerelle, & Hildebrand, 2002). Significantly enhanced cell–material interactions are reported on nanophase ceramics compared to microphase ceramics (Webster, Ergun, Doremus, Siegel, & Bizios, 2000). Therefore, continuous efforts are being made to engineer biomaterials/particles in nanoscale topography/size. Recently, bioactive glass ceramic has been synthesized

\* Corresponding author. Tel.: +91 484 2801234; fax: +91 484 2802020.

E-mail addresses: [rjayakumar@aims.amrita.edu](mailto:rjayakumar@aims.amrita.edu), [jayakumar77@yahoo.com](mailto:jayakumar77@yahoo.com) (R. Jayakumar).

as nanoparticles (nBGC) by sol-gel process (Xia & Chang, 2007). Hence it is interesting to investigate the possibility of preparing a scaffold using chitosan matrix disseminated with nBGC to evaluate the influence of nBGC addition in scaffold properties for tissue engineering applications. Therefore in this paper, we address the preparation of chitosan/nBGC composite scaffolds and its properties relevant to tissue engineering applications.

## 2. Experimental

### 2.1. Materials

Chitosan (Degree of deacetylation – 85%) was purchased from Koyo Chemical Co Ltd (Japan). Tetraethyl orthosilicate (TEOS), calcium nitrate ( $\text{Ca}(\text{NO}_3)_2 \cdot 4\text{H}_2\text{O}$ ), citric acid, ammonium dibasic phosphate, sodium borohydride, acetic acid, sodium hydroxide, Alpha minimum essential medium ( $\alpha$ -MEM), and 3-(4,5-dimethylthiazol-2-yl)-2,5-diphenyltetrazolium bromide MTT, were purchased from Sigma Aldrich Company. Glutaraldehyde and hen lysozyme was purchased from Fluka. Trypsin-EDTA and fetal bovine serum (FBS) were obtained from Gibco, Invitrogen Corporation.

### 2.2. Preparation of nanocomposite scaffolds

Two percentage (w/v) CS was dissolved in 1% acetic acid solution. Bioactive glass ceramic nanoparticles (nBGC) (size – 100 nm) were prepared as previously reported (Peter et al., in press). Then 1 wt.% of nBGC was added into chitosan solution and stirred for 24 h. Resultant solution was subjected to ultrasonication to reduce particle size and fine dispersion. To this solution, 0.25% glutaraldehyde was added as cross linker. The resultant solution was transferred into 12 well plates (BD Biosciences) and pre-frozen at  $-20^\circ\text{C}$  for 12 h followed by freeze-drying (Christ alpha LD plus) at  $-80^\circ\text{C}$  for 48 h. After that, the composite scaffolds were neutralized by 2% NaOH & 5% NaBr for 2 h and washed with deionised water. The resultant scaffolds were freeze-dried and stored for further use.

### 2.3. Characterizations

#### 2.3.1. Electron microscopy studies

The structural morphology of the composite scaffolds were examined using scanning electron microscope (SEM). Composite scaffold samples were prepared by taking thin sections with a ra-

zor blade. The sections were platinum sputtered in vacuum (JEOL, JFC-1600, Japan), and examined using scanning electron microscope (JEOL, JSM-6490LA, Japan). The average pore size was determined by measuring the size of randomly selected 30 pores.

#### 2.3.2. FT-IR studies

FT-IR spectra of composite scaffolds were characterized using a FTIR spectrometer (Perkin-Elmer RX1). Dried composite scaffolds were ground and mixed thoroughly with potassium bromide at a ratio of 1:5 (Sample: KBr). The IR spectra were then analyzed using Perkin-Elmer RX1 operating at range of  $400\text{--}4000\text{ cm}^{-1}$ .

#### 2.3.3. XRD studies

XRD patterns of composites scaffolds were obtained at room temperature using a Panalytical XPERT PRO powder diffractometer ( $\text{Cu K}\alpha$  radiation) operating at a voltage of 40 kV. XRD was taken at  $2\theta$  angle range of  $5\text{--}60^\circ$  and the process parameters were: scan step size  $0.02 (2\theta)$  and scan step time 0.05 s.

### 2.4. Swelling studies

The swelling studies were performed in PBS at pH 7.4 at  $37^\circ\text{C}$ . The dry weight of the scaffold was noted ( $W_o$ ). Scaffolds were placed in PBS buffer solution at pH 7.4 for 1 h and removed. The surface adsorbed water was removed by filter paper and wet weight was recorded ( $W_w$ ). The ratio of swelling was determined by the following formula.

$$\text{Swelling Ratio} = W_w - W_o / W_o$$

### 2.5. Density studies

To determine the density of scaffold, three scaffolds were selected and measurement was performed on an analytical balance equipped with a density determination kit (Sartorius YDK 01). Density measurements were done with ethanol as the displacement medium. Ethanol did not cause a change in pore size hence used as displacement medium.

### 2.6. In-vitro degradation studies

Degradation of the composite scaffold was studied in PBS medium containing lysozyme at  $37^\circ\text{C}$ . Three scaffolds were immersed in lysozyme (10,000 U/ml) containing medium and incubated at

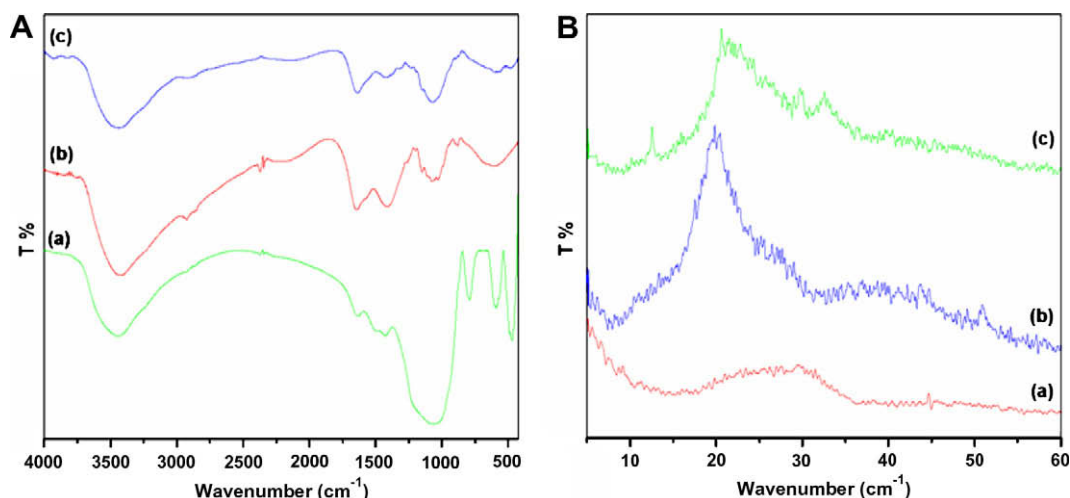


Fig. 1. FT-IR spectra (A) & XRD pattern (B) of nBGC (a), CS (b) and CS/nBGC (c) scaffolds.

37 °C for 7 days. Initial weight of the scaffold was noted as  $W_0$  and after 7 days the scaffold was washed in deionised water to remove ions adsorbed on surface and freeze dried. The dry weight was noted as  $W_t$ . The degradation of scaffold was calculated using the following formula.

$$\text{Degradation \%} = W_0 - W_t / W_0 \times 100$$

## 2.7. In-vitro biomineralization studies

Three composite scaffolds of equal weight and shape was immersed in  $1 \times$  simulated body fluid (SBF) (Kokubo & Takadama, 2006) solution and then incubated at 37 °C in closed falcon tube for 7 days. After specified time, scaffolds were removed and washed three times with deionised water to remove adsorbed minerals. Then the scaffolds were lyophilized, sectioned and viewed using SEM for mineralization.

## 2.8. Cell culture studies

Cell studies were conducted using osteoblast like cells (MG-63). Cell lines were maintained in the cell culture facility in MEM with 10% FBS and 100 U/ml penicillin–streptomycin. Cells were detached from the culture plate at 80–85% confluency and used for seeding on the scaffolds for investigating the cytocompatibility of composite scaffolds. Prior to cell seeding, scaffolds were sterilized using ethanol/UV treatment and incubated with culture medium for 1 h at 37 °C in a humidified incubator with 5% CO<sub>2</sub> and 85% humidity. Cells were seeded drop wise onto the top of the scaffolds ( $1 \times 10^5$  cells/100  $\mu$ l of medium/scaffold), which fully absorbed the media, allowing cells to distribute throughout the scaffolds. Subsequently, the cell-seeded scaffolds were kept at 37 °C in a humidified incubator under standard culturing conditions for 4 h in order to allow the cells to attach to the scaffolds. After 4 h, scaffolds were fed with additional culture medium.

### 2.8.1. Cytocompatibility of the scaffolds

The viability of cells grown on the scaffolds was determined using the colorimetric MTT assay. MTT assay measures the reduction of the tetrazolium component MTT by viable cells. Therefore, the level of reduction in MTT into formazan can reflect the level of cell metabolism. For the assay, cells were seeded on 96 well plates at a density of  $10^4$  cells/well and were incubated under standard culturing conditions. Extract from the scaffolds were prepared by incubating the pre-sterilized scaffolds incubated in culture medium as per ISO specification 10993-5 (i.e. 60 cm<sup>2</sup> per 20 ml of medium for 24 h at 37 °C with agitation) and the medium with

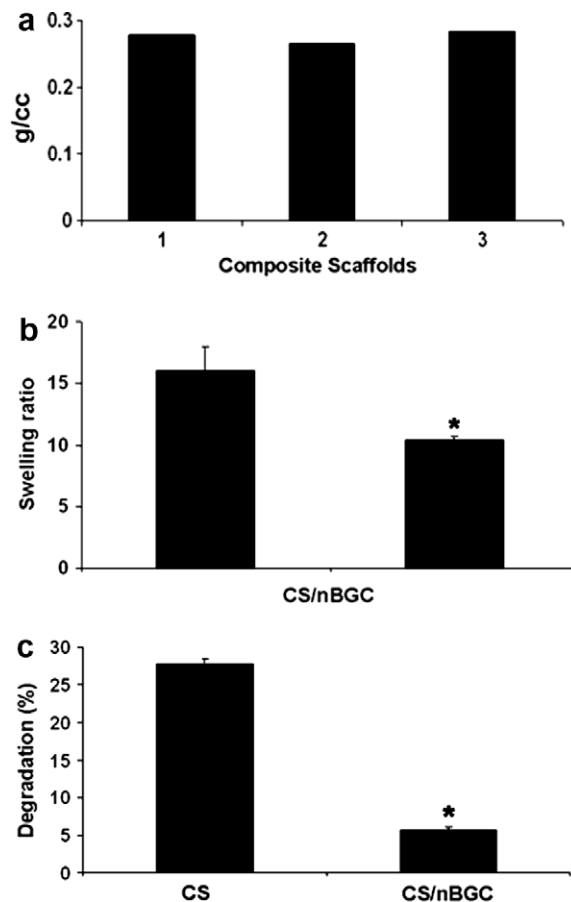


**Fig. 3.** (a) Density of the CS (1) and composite scaffolds (2 & 3) compared to CS scaffolds. (b) Swelling behaviour of the scaffolds, which showed that addition of nBGC, decreased the swelling in composite scaffolds compared to CS scaffolds. \* $p < 0.05$ . (c) *In-vitro* degradation studies in lysozyme, which showed significant, decrease in degradation rate in composite scaffolds compared CS scaffolds. \* $p < 0.05$ .

leachables was collected in a falcon tube. Culture media of the seeded cells were replaced after 24 h by the extract (media with the leachables). Cells were incubated on the extract for 24 h. After the incubation period, the extract was replaced by fresh media containing 10% of MTT solution. After that, plate was incubated at 37 °C in humidified atmosphere for 4 h. Then the medium was removed, 100  $\mu$ l of solubilization buffer (Triton-X100, 0.1 N HCl and isopropanol) was added to each well to dissolve the formazan

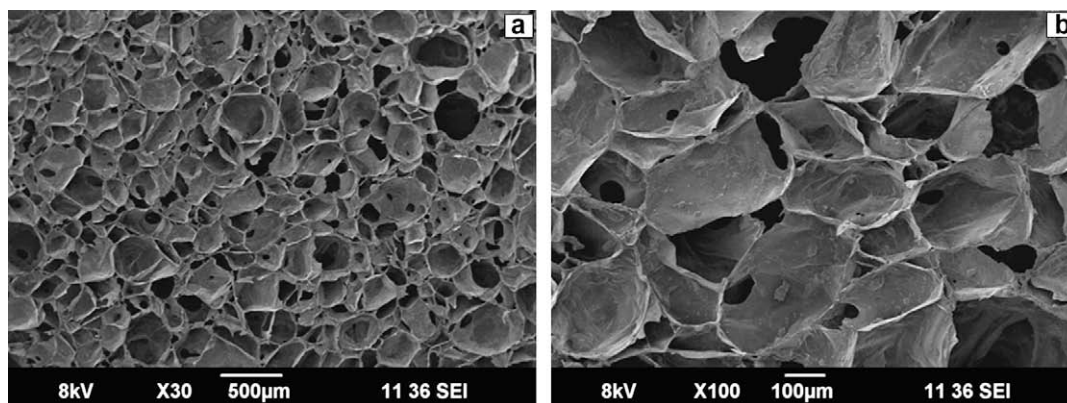


**Fig. 2.** (a) SEM images showing the macro porous microstructure of composite scaffold. Pore size ranged from 150 to 300  $\mu$ m & nBGC particles were on the chitosan matrix (b).

crystals. The absorbance of the lysate was measured in a microplate reader (biotek) at a wavelength of 570 nm.

Direct contact test was performed to show cytocompatibility of the scaffolds placed in direct contact with cells. Cells were grown as monolayer on culture dishes and pre-sterilized scaffolds were placed and incubated for 24 h in direct contact to monolayer of cells. After the incubation period, scaffolds were removed from the monolayer of cells and images of the monolayer of cells were acquired with an inverted microscope (Leica) attached with a CCD camera.

### 2.8.2. Cell morphology on the scaffolds

Morphology and spreading pattern of cells on the scaffolds were evaluated 12 and 24 h after seeding using SEM. For SEM analysis, cell-seeded scaffolds were fixed with 2.5% glutaraldehyde, rinsed with PBS and dehydrated using graded series of ethanol (25–100%). The samples were coated with platinum and examined under SEM.

### 2.9. Statistical analysis

All quantitative results were obtained from triplicate samples. Data was expressed as Mean  $\pm$  SD ( $n = 3$ ). Statistical analysis was carried out using Student's two-tailed  $t$  test. A value of  $p < 0.05$  was considered to be statistically significant.

## 3. Results and discussion

### 3.1. Characterizations

#### 3.1.1. FT-IR studies

FT-IR spectra of CS/nBGC (Fig. 1A) showed a peak at  $1649\text{ cm}^{-1}$ , which corresponds to the primary amine groups of chitosan. The peak at  $1030\text{ cm}^{-1}$ , which is attributed to phosphate groups, was

also present in CS/nBGC scaffolds. In comparison to CS, CS/nBGC scaffolds were characterized by three absorption bands at  $602$  and  $564\text{ cm}^{-1}$ , corresponding to the stretching vibration bands of P–O from  $\text{PO}_4^{3-}$  and  $467\text{ cm}^{-1}$  assigned to Si–O–Si bending mode.

#### 3.1.2. XRD studies

The XRD analysis of the composite scaffolds (Fig. 1B) showed a peak at  $21^\circ$ , which is attributed to CS in the scaffold. This confirmed that the calcined glass generally existed in amorphous state and no diffraction peaks could be observed except a broad band between  $15^\circ$  and  $40^\circ$  ( $2\theta$ ) (Xia & Chang, 2007).

#### 3.1.3. SEM and density studies

SEM micrograph of composite scaffolds (Fig. 2) showed that scaffolds were macro porous in nature. Pore size of CS/nBGC scaffold varied from  $150\text{--}300\text{ }\mu\text{m}$  as measure by SEM. Pores are necessary in bone tissue engineering for the migration and proliferation of osteoblasts and mesenchymal cells, as well as vascularization. Compared to CS scaffolds, density of the composite scaffolds decreased with the addition of nBGC (Fig. 3a). This may be due to the increase in porosity of the composite scaffolds due to the addition of nanoparticles.

### 3.2. Swelling studies

Swelling behaviour of the scaffolds was as shown in (Fig. 3b). The composite scaffolds showed significantly decreased swelling ratio compared to CS scaffolds. Swelling causes an increase in the pore size and porosity, which aids in the supply of nutrients and oxygen to the interior regions of the composite scaffolds. However, scaffold's uncontrolled swelling can be detrimental for tissue engineering applications. Our results suggest that, by adding nBGC to CS scaffolds it is possible to control the swelling behaviour of CS scaffolds.

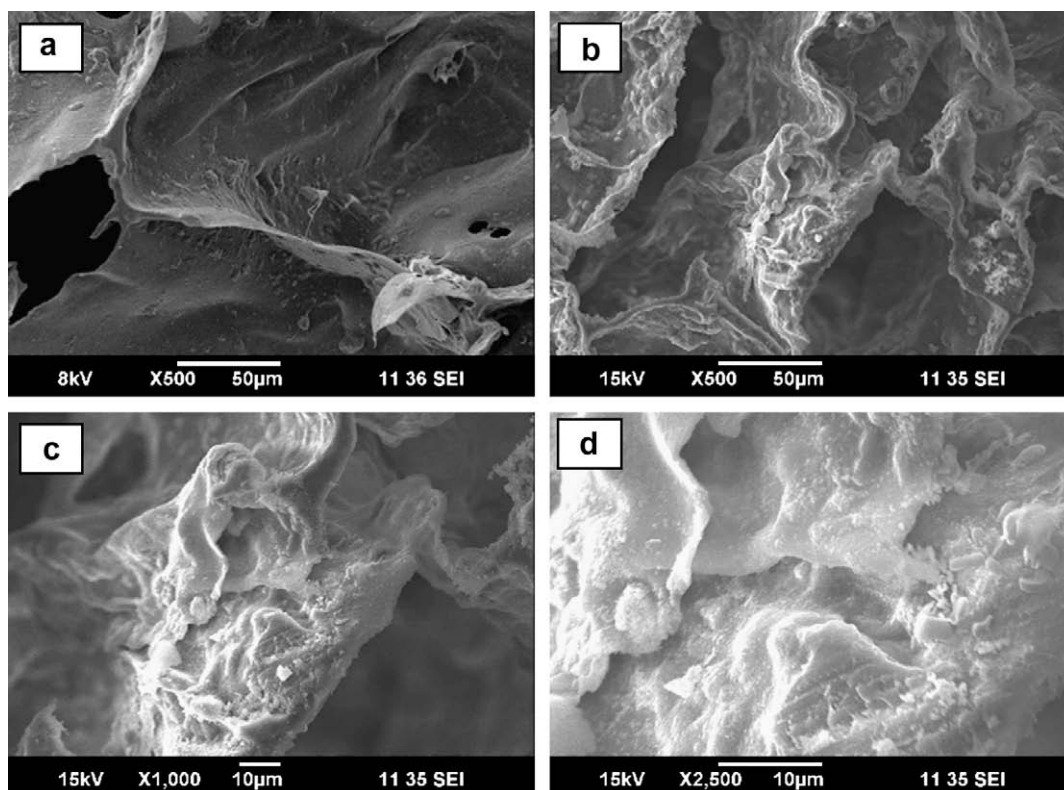


Fig. 4. In-vitro biomineralization studies on the composite scaffolds after 7 days. (a) CS/nBGC and (b–d), mineralized CS/nBGC composite scaffolds.



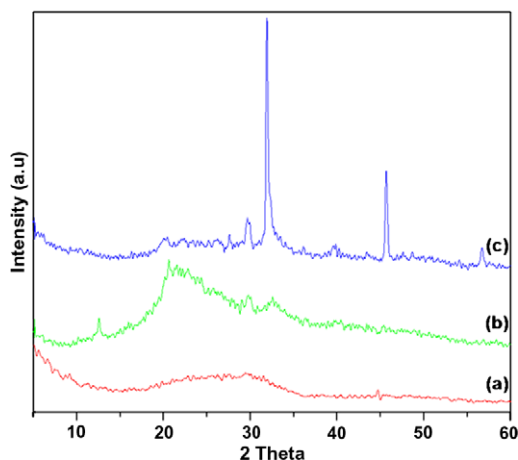


Fig. 5. XRD spectra of (a) nBGC, (b) CS/nBGC and (c) CS/nBGC composite scaffold after soaking 7 days in SBF solution.

### 3.3. Biodegradation studies

The *in-vitro* biodegradation of scaffolds after 1 week of immersion in PBS showed significant difference in the degradation rate of nanocomposite scaffolds compared to CS scaffolds (Fig. 3c). CS/nBGC composite scaffolds showed significant decline in the degradation rate compared to pristine chitosan scaffolds. Degradation of chitosan can result in acidic degradation products, which may be neutralized by alkali groups leaching out from bioglass thus reducing the degradation rate. Moreover the activity of lysozyme is quicker at acidic pH (Nordtveit, Varum, & Smidsrod, 1996).

### 3.4. *In-vitro* biomineralization studies

*In-vitro* biomineralization studies showed the deposition of minerals on the surface of composite scaffolds after 7 days incubation in SBF solution (Fig. 4). The XRD study also confirms the min-

eral deposition on scaffolds, which reflected as a sharp peak at  $31.7^\circ$  attributed to hydroxyapatite (Jayakumar et al., 2009; Madhupathi et al., 2009a, 2009b, 2009c) (Fig. 5). These results confirm the bioactive nature of the composite scaffolds.

### 3.5. Cell studies

The MTT assay results showed that there was no significant decrease in the optical density (OD) values in cells treated with extract (Fig. 6a). This suggests that the developed scaffolds have no cytotoxic leachables therefore it is cytocompatible. The direct contact test results showed that, cells retained characteristic morphology of MG-63 cell line when cultured in direct contact with composite scaffolds (Fig. 6b). This result also suggests that the composite scaffolds are cytocompatible and can be used for tissue engineering applications.

SEM was used to study the attachment and spreading of cells to the scaffolds. Cells were found to be attached to the pore walls offered by the composite scaffolds after 12 h and became spread after 24 h (Fig. 7). These results suggest that cells could attach and spread well on the composite scaffolds.

## 4. Conclusions

Nanocomposite scaffolds were prepared using nBGC disseminated chitosan matrix by lyophilization technique. The prepared composite scaffolds were characterized using FT-IR, SEM, XRD and EDS studies. In addition, swelling, density, degradation, bioactivity, cytotoxicity and cell attachment studies of the composite scaffolds were also performed. The macro porous scaffolds showed interconnected pores (150–300  $\mu\text{m}$ ) in the nanoparticles dispersed chitosan matrix. The developed composite scaffolds showed controlled swelling and degradation by the addition of nBGC. Bioactivity studies showed that the prepared composite scaffolds were bioactive. Cells seeded on the composite scaffolds attached to the pore walls of the scaffolds and spread overtime. The scaffolds were also found to be cytocompatible in MTT assay and no morphological

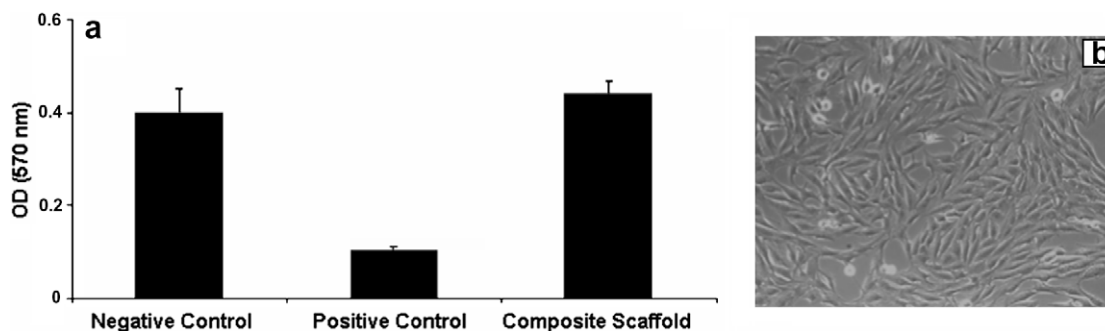


Fig. 6. (a) MTT assay showing biocompatibility of the composite scaffolds. (b) The morphology of cells grown in direct contact with composite scaffolds.

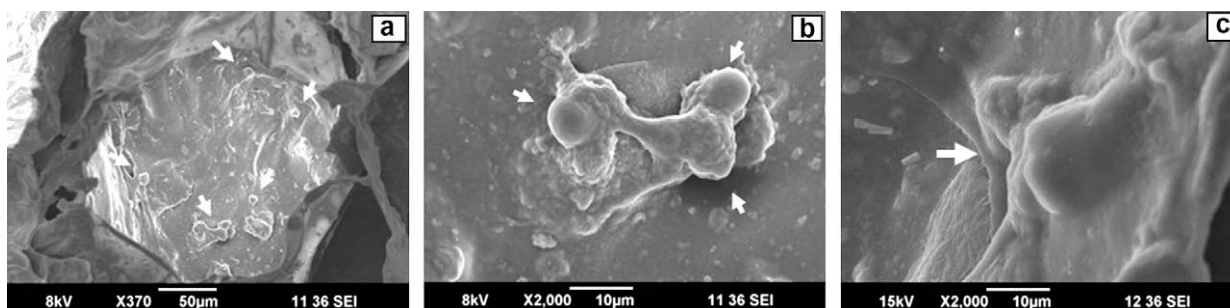


Fig. 7. The SEM image of MG-63 cells attached to composite scaffolds. (a) Cells attached to the pore walls at 12 h (arrows). (b) Higher magnification image showing initial signs of cell spreading 12 h and (c) 24 h.

changes were observed to cells grown in direct contact with the scaffolds. Therefore we concluded that the CS/nBGC nanocomposite scaffolds are potential scaffolds for tissue engineering applications.

## Acknowledgements

The Department of Science and Technology, Government of India supported this work, under a centre grant of the Nanoscience and Nanotechnology Initiative program monitored by Dr. C.N.R. Rao. The authors are thankful to Prof. Greta R. Patzke, Institute of Inorganic Chemistry, University of Zurich for helping in TEM studies. The authors are also thankful to Mr. Sajin. P. Ravi for his help in SEM studies. One of the authors N. S. Binulal gratefully acknowledged to Council of Scientific and Industrial Research (CSIR), Government of India for providing Senior Research Fellowship (SRF).

## References

- Bosetti, M., & Cannas, M. (2005). The effect of bioactive glasses on bone marrow stromal cells differentiation. *Biomaterials*, 26, 3873–3879.
- Cao, W., & Hench, L. L. (1996). Bioactive materials. *Ceramics International*, 22, 493–507.
- Dalby, M. J., McCloy, D., Robertson, M., Wilkinson, C. D. W., & Oreffo, R. C. (2006). Osteoprogenitor response to defined topographies with nanoscale depths. *Biomaterials*, 27, 1306–1315.
- Foppiano, S., Marshall, S. J., Marshall, G. W., Saiz, E., & Tomsia, A. P. (2007). Bioactive glass coatings affect the behaviour of osteoblast-like cells. *Acta Biomaterialia*, 3, 765–771.
- Gupta, P. N., Mahor, S., Khatri, K., Goyal, A., & Vyas, S. P. (2006). Phospholipid vesicles containing chitosan nanoparticles for oral immunization; Preparation and in-vitro investigation. *Asian Chitin Journal*, 2, 91–96.
- Hirano, S., Itakura, C., Seino, H., Akiyama, Y., Nonaka, I., Kanbara, N., et al. (1990). Chitosan as an ingredient for domestic animal feeds. *Journal of Agricultural and Food Chemistry*, 38, 1214–1217.
- Jayakumar, R., Reis, R. L., & Mano, J. F. (2006). Chemistry and applications of phosphorylated chitin and chitosan. *E-Polymers*, 035.
- Jayakumar, R., Nwe, N., Tokura, S., & Tamura, H. (2007). Sulfated chitin and chitosan as novel biomaterials. *International Journal of Biological Macromolecules*, 40, 175–181.
- Jayakumar, R., Prabakaran, M., Reis, R. L., & Mano, J. F. (2005). Graft copolymerised chitosan – present status and applications. *Carbohydrate Polymers*, 62, 142–158.
- Jayakumar, R., Rajkumar, M., Freitas, H., Sudheesh Kumar, P. T., Nair, S. V., Furuike, T., et al. (2009). Bioactive and metal uptake studies of carboxymethyl chitosan-graft-d-glucuronic acid membranes for tissue engineering and environmental applications. *International Journal of Biological Macromolecules*, 45, 135–139.
- Jayakumar, R., Selvamurugan, N., Nair, S. V., Tokura, S., & Tamura, H. (2008). Preparative methods of phosphorylated chitin and chitosan – an overview. *International Journal of Biological Macromolecules*, 43, 221–225.
- Jayakumar, R., & Tamura, H. (2006). Apatite forming ability of N-carboxymethyl chitosan gels in a simulated body fluid. *Asian Chitin Journal*, 2, 61–68.
- Jiang, T., Nair, L. S., & Laurencen, C. T. (2006). Chitosan composites for tissue engineering: Bone tissue engineering scaffolds. *Asian Chitin Journal*, 2, 1–10.
- Kokubo, T., & Takadama, H. (2006). How useful is SBF in predicting in-vivo bone activity? *Biomaterials*, 27, 2907–2915.
- Kong, L., Gao, Y., Cao, W., Gong, Y., Zhao, N., & Zhang, X. (2005). Preparation and characterization of nano-hydroxyapatite/chitosan composite scaffolds. *Journal of Biomedical Material Research*, 75A, 275–282.
- Lauer, G., Wiedmann-Al-Ahmad, M., Otten, J. E., Hubner, U., Schmelzeisen, R., & Schilli, W. (2001). The titanium surface texture effects adherence and growth of human gingival keratinocytes and human maxillar osteoblast-like cells in vitro. *Biomaterials*, 22, 2799–2809.
- Linez-Bataillon, P., Monchau, F., Bigerelle, M., & Hildebrand, H. F. (2002). In vitro MC3T3 osteoblast adhesion with respect to surface roughness of Ti6Al4V substrates. *Biomolecular Engineering*, 19, 133–141.
- Madhumathi, K., Binulal, N. S., Nagahama, H., Tamura, H., Shalumon, K. T., Selvamurugan, N., et al. (2009a). Preparation and characterization of novel  $\beta$ -chitin-hydroxyapatite composite membranes for tissue engineering applications. *International Journal of Biological Macromolecules*, 44, 1–5.
- Madhumathi, K., Shalumon, K. T., Divya Rani, V. V., Tamura, H., Furuike, T., Selvamurugan, N., et al. (2009b). Wet chemical synthesis of chitosan hydrogel-hydroxyapatite composite membranes for tissue engineering applications. *International Journal of Biological Macromolecules*, 45, 12–15.
- Madhumathi, K., Sudheesh Kumar, P. T., Kavya, K. C., Furuike, T., Tamura, H., Nair, S. V., et al. (2009c). Novel chitin/nanosilica composite scaffolds for bone tissue engineering applications. *International Journal of Biological Macromolecules*, 45, 289–292.
- Muzzarelli, R. A. A. (2009). Chitins and chitosans for the repair of wounded skin, nerve, cartilage and bone. *Carbohydrate Polymers*, 76, 167–182.
- Muzzarelli, R. A. A., Baldassare, V., Conti, F., Ferrara, P., Biagini, G., Gazanelli, G., et al. (1988). Biological activity of chitosan: Ultrastructural study. *Biomaterials*, 9, 247–252.
- Nordtveit, R. J., Varum, V. M., & Smidsrod, O. (1996). Degradation of partially N-acetylated chitosans with hen egg white and human lysozyme. *Carbohydrate Polymers*, 29, 163–167.
- Oliva, A., Salerno, A., Locardi, B., Riccio, V., Ragione, F. D., Iardino, P., et al. (1998). Behaviour of human osteoblasts cultured on bioactive glass coatings. *Biomaterials*, 19, 1019–1025.
- Peter, M., Sudheesh Kumar, P. T., Binulal, N. S., Nair, S. V., Tamura, H., & Jayakumar, R. (2009). Development of novel  $\alpha$ -chitin/nano bioactive glass ceramic composite scaffolds for tissue engineering applications. *Carbohydrate Polymers*, 78, 926–931.
- Takahashi, Y., Yamamoto, M., & Tabata, Y. (2005). Osteogenic differentiation of mesenchymal stem cells in biodegradable sponges composed of gelatin and  $\beta$ -tricalcium phosphate. *Biomaterials*, 26, 3587–3596.
- Verrier, S., Blaker, J. J., Maquet, M., Hench, L. L., & Boccaccinia, R. A. (2004). PDLLA/bioglass composites for soft-tissue and hard-tissue engineering: An in vitro cell biology assessment. *Biomaterials*, 25, 3013–3021.
- Webster, T. J., Ergun, C., Doremus, R. H., Siegel, R. W., & Bizios, R. (2000). Enhanced functions of osteoblasts on nanophase ceramics. *Biomaterials*, 21, 1803–1810.
- Xia, W., & Chang, J. (2007). Preparation and characterization of nano-bioactive-glasses (NBG) by a quick alkali-mediated sol–gel method. *Materials Letters*, 61, 3251–3253.
- Xynos, I. D., Edgar, A. J., Buttery, L. D. K., Hench, L. L., & Polak, J. M. (2000). Ionic products of bioactive glass dissolution increase proliferation of human osteoblasts and induce insulin-like growth factor II mRNA expression and protein synthesis. *Biochemical and Biophysical Research Communication*, 276, 461–465.
- Yin, Y., Ye, F., Chu, J., Zhang, F., Li, X., & Yao, K. (2003). Preparation characterization of macroporous chitosan-gelatin/ $\beta$ -tricalcium phosphate composite scaffolds for bone tissue. *Journal of Biomedical Material Research*, 67A, 844–855.
- Zhang, Y., Venugopal, J. R., El-Turki, A., Ramakrishna, S., Su, B., & Lim, C. T. (2008). Electrospun biomimetic nanocomposite nanofibers of hydroxyapatite/chitosan for bone tissue engineering. *Biomaterials*, 29, 4314–4322.
- Zhao, F., Grayson, W. L., Ma, T., Bunnell, B., & Lu, W. W. (2006). Effects of hydroxyapatite in 3-D chitosan-gelatin polymer network on human mesenchymal stem cell construct development. *Biomaterials*, 27, 1859–1867.
- Zheng, J. P., Wang, C. Z., Wang, X. X., Wang, H. Y., Zhuang, H., & Yao, K. D. (2007). Preparation of biomimetic three-dimensional gelatin/montmorillonite-chitosan scaffold for tissue engineering. *Reactive and Functional Polymers*, 67, 780–788.